A Visible Light Communication based predictive system for the height and location estimation of an obstacle

Aranya Chakraborty*, Anand Singh+, Vivek Ashok Bohara+, and Anand Srivastava+
*Indian Institute of Science, Bengaluru, India, 560012
+IIIT-Delhi, New Delhi, India, 110020

This paper presents a visible light communication (VLC) - based predictive system for estimating an obstacle's height and location in an indoor environment. Two types of indoor environments having one and four LED's respectively are considered for the simulation. In each of the above environments, the system is first simulated using an infinitely thin obstacle and then using an obstacle having a radius of 0.05m. Linear Regression is applied to the results to develop a predictive algorithm to obtain the location and height of an obstacle from the received power profile. Finally, the accuracy of the predictive system for each of the above scenarios is also measured.

***Index Terms*—Visible Light Communication, Indoor positioning, Machine learning (ML), Light-emitting-diodes LEDs.**

I. INTRODUCTION

There has been a recent increase in the popularity of location-based services due to developments in wireless sensor networks and physical networking technology. Indoor positioning garners much attention due to its wide application spectrum, including large shopping malls, underground parking, lofts and storage spaces, etc. Several indoor positioning technologies, such as those based on assisted global positioning system (A-GPS), a pseudo-satellite (Pseudo lite), wireless local area network (WLAN), radio frequency tags (RFID), Zigbee, Bluetooth (BT), ultra-wideband radio (UWB), infrared, computer vision, magnetic, ultrasonic, and visible light, are being looked into to achieve high-precision indoor navigation [1] [2] [3] [4]. However, GPS positioning is not suitable for indoor systems due to the building Walls, which result in high path loss. Due to high attenuation in air, UWB based positioning is also not suitable for large indoor environments. WLAN positioning uses a fingerprint library method for positioning, which is complicated to set up, and the positioning accuracy is also relatively low [5]. Other positioning methods, such as infrared, Zigbee, and Bluetooth, are vulnerable to fluctuations in signal sources [6]. In light of these indoor positioning systems' shortcomings, [7] Visible Light-based position emerges as a viable alternative. From the practical point of application, the LED-based visible light positioning (VLP) system has great potential. In a VLP system, LEDs are used as transmitters, and photodetectors are commonly used at the receiver end for visible light localization [8].Yoshino proposed a positioning system based on a visible light image sensor [9].

Visible light communication (VLC) is a relatively new technology that recently became the subject of exploration within the academic and industrial research for indoor positioning [10]. It offers high bandwidth, high positioning accuracy, and immunity from electromagnetic interference's [11]. It can also be used without a prior license. Moreover, no large scale changes are required as they can be integrated seamlessly within the existing infrastructure. The two primary components of the VLC-based indoor positioning are: LED transmitters and photodiode (PD) optical receivers. LED transmitters are installed at fixed locations inside a room and continuously transmit their position coordinates encoded as an optical signal. The LED's transmitted optical signals are affected by multipath propagation, shadowing, and interference from various noise sources. Thus, a considerable amount of research has been done to find suitable implementation techniques for the VLC based indoor positioning system (IPS) to achieve high positioning accuracy [12]. Based on received signal strength (RSS), a simple regression-based approach with linear and nonlinear least square estimations (LLS & NLS) have been shown in [13]. The regression approach's performance is evaluated by different metrics such as the average, standard deviation, and cumulative distribution function of the localization error. A key conclusion of this work is that using the regression method enhances the VLC indoor positioning system's performance.

This paper aims to test the accuracy of RSS-based positioning in determining an obstacle's height and location in an indoor environment. This is done by developing a predictive system using simulations and Linear Regression. In the first part, the system is simulated using a single object of negligible width (essentially a line).In the second part, the system is simulated using a single object with a finite radius. The simulation's radius is taken as constant (=0.05m). The results obtained from the simulation are used to develop a predictive system with the Linear Regression algorithm. The predictive system then provides an obstacle's height and location based on the resultant Received Power Profile. Though indoor positioning using VLC is an established area of study, this paper's novel feature is constructing an algorithm that calculates the blockage's height and location based on RSS. Such an algorithm can be used in an indoor environment to remotely construct a 3d model of a room using a relatively cheap apparatus consisting of LEDs and optical photodiodes. The model can also be easily expanded to include multiple obstacles and dynamic obstacles and can be used for surveillance and monitoring in an indoor environment.

The rest of the paper is organized as follows. Section II presents the system model for the proposed VLC based

predictive system with the VLC channel model, spatial model, simulation model, and regression model. The obtained simulation results have been discussed in Section III. Finally, Section IV concludes the paper.

II. System Model

As mentioned before, we consider two setups of 1 and 4 LEDs in an indoor environment of a $5\ \mathrm{m} \times 5\ \mathrm{m} \times 3\ \mathrm{m}$ room. In the single LED setup, the LED is placed at the ceiling's centre, whereas for the four LED configuration, the LED's are at the midpoints of the diagonals from the centre to the vertices. The Received Power profiles in the absence of an obstacle for both the setups can be seen in Fig 1(a) and Fig 1(b), respectively.

In the following subsections, we discuss in detail the VLC channel model,the spatial model of the obstacles, the simulation model and the regression model used.

A. VLC Channel Model

Lambert radiator is a typical radiation model that can model the LED light source in VLC [14]. Radiation patterns of few commercially available LEDs are assumed to be Lambertian. $H(0)$ is the channel gain of LoS component, which is given as:

$$H(0) = \begin{cases} \dfrac{(m+1)A}{2\pi D_d^2} \cos^m(\phi) T_s(\psi) g(\psi) \cos(\psi) \\ \qquad\qquad 0 \le \psi \le \psi_c \ , \end{cases} \tag{1}$$

where m represents Lambertian order defined as:

$$m = \frac{-ln(2)}{ln(cos(\phi_{\frac{1}{2}}))} \ . \tag{2}$$

In (1), A is the physical area of the PD, D_d is the distance between the VLC transmitter and the receiver, ψ is the angle of incidence, ϕ is the angle of irradiance, ψ_c is the receiver field of view (FOV), $T_s(\psi)$ is the gain of the optical filter, and $g(\psi)$ is the gain of the optical concentrator given as:

$$g(\psi) = \begin{cases} \dfrac{n^2}{\sin^2(\psi_c)}, & 0 \le \psi \le \psi_c, \end{cases} \tag{3}$$

where n is the refractive index of optical concentrator and $\phi_{\frac{1}{2}}$ is LED half beam angle.

B. Spatial Model

Consider the scenario illustrated in Fig. 2, where a transmitter (Tx) is located at a certain height h_T above the ground. As stated before, we model the blockages as cylinders [15] with a certain height, h_B, and the base diameter of r. For the purpose of simulations, two different types of obstacles are considered in this paper. In the first part, an infinitely thin obstacle is considered, which is represented by the black line in Figure 2. An infinitely thin object can be considered as a line of a certain height and is a purely theoretical construct. In the second part, an obstacle having some finite radius, here taken to be constant and equal to 0.05m, is considered. The blue diffused region represents such an object in Figure 2 and is much closer to real-life obstacles.

As illustrated in Fig 2, a blockage of height h_B present between the LED and the receiver, results in a communication link blockage. The distance of the blockage and the receiver from LED is denoted by d_B and d_T, respectively.

C. Simulation Model

The room floor, which is (5×5) m, is assumed to be a Cartesian plane spanning from -2.5 to 2.5 on both the axes with a least count of 0.1 m. The centre of the room is assumed to be the Origin. The obstacle's location is simulated by taking two random values in the span of (-2.5,2.5) as the X and Y coordinates. The height of the obstacle is taken to be a random value between 4'8" and 6'4" feet, which is assumed to be the approximate range of human height. The simulation is then carried out 1000 times using the VLC channel model with the constants' value given in Table 1, each time taking an obstacle at a random location and of a random height, and the resultant received power profile (RPP) is recorded. Thus, the 1000 data points are then divided roughly into a training set and a test set in a roughly 4:1 ratio. The training set is used to train the linear regression algorithm and obtain predictive parameters. The test set is then used to calculate the accuracy of the predictive parameters by using them to predict the obstacle's height and location from the resultant RPP and comparing them to the actual values.

TABLE I
System model Parameters

Parameter	Value
Room size	$5\ \mathrm{m} \times 5\ \mathrm{m} \times 3\ \mathrm{m}$
LED transmitted power	20 mw
Refractive index n	1.5
Optical filter gain T_s	1
LED irradiance angle	$56°$
Receiver elevation	$90°$
Receiver active area	$1\ \mathrm{cm}^2$
Field of views (FOVs) of receiver	$70°$.
Blockage radius	0.05 m
Responsivity ($\mathcal{R}$)	$0.5\ \frac{\mathrm{A}}{\mathrm{W}}$
Signal bandwidth B_s	10 MHz
Noise bandwidth factor I_2	0.562
Background current I_{bg}	100 μA

D. Regression Model

The training set is used to train the linear regression algorithm and obtain the predictive parameters. In this paper, we have used the standard Multivariate Linear Regression model, where the hypothesis function is given by (4), and the cost function is given by (5). Here, **X** is a matrix that contains values derived from the difference between the RPP with and without the obstacle given in Figure 5-8(b). It includes the distance and the coordinates of the point at which the value is maximum and the shadow's length. **Y** is a matrix containing the actual value of the obstacle's height and location, and θ is a matrix representing the predictive parameter, and its initial value is taken as zero.

$$h_\theta(x) = \theta^T \times X = \theta_0 x_0 + \theta_1 x_1 + \theta_2 x_2 + ... + \theta_n x_n \tag{4}$$

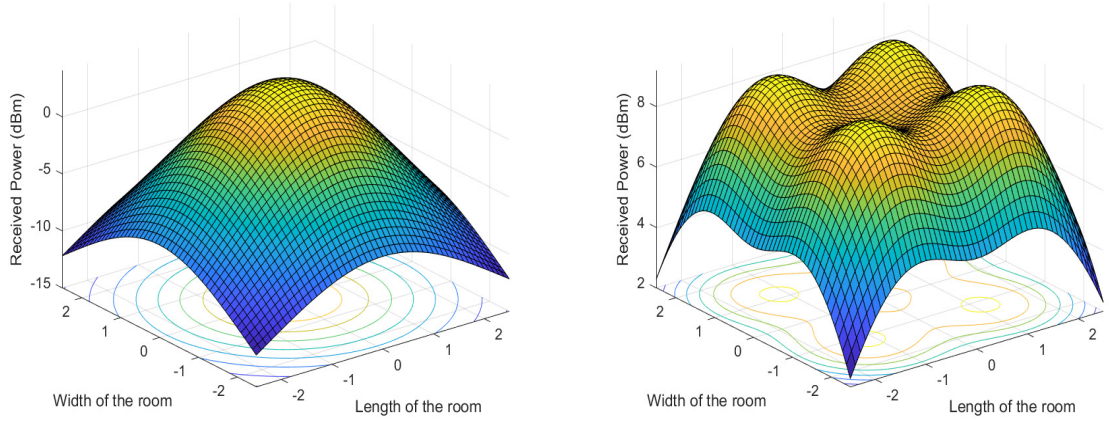

(a) Single LED setup

(b) Four LED setup

Fig. 1. Received Power Profiles without obstacle

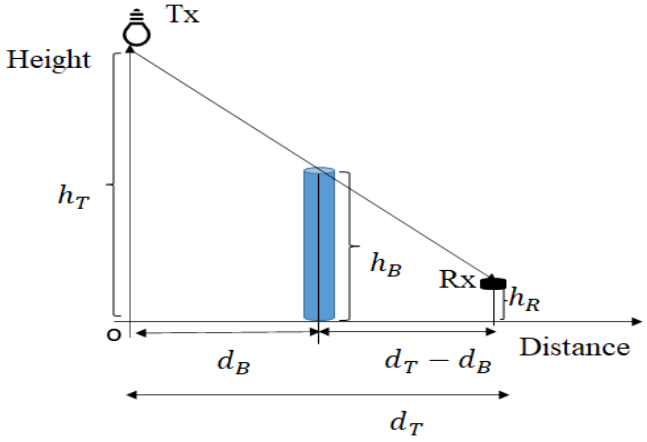

Fig. 2. Schematic for calculation of shadow length due to blockage

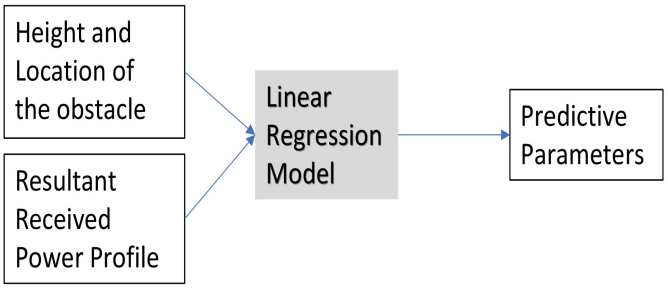

Fig. 3. Parameter training using Linear Regression

$$J(\theta_0, \theta_1, ..., \theta_n) = \frac{1}{2m} \sum_{i=1}^{m} [h_\theta(x^i) - y^i]^2 \qquad (5)$$

After **X** and **Y** are obtained from the simulation, gradient descent, given in algorithm 1 where α is the learning rate, is used to find the value of θ for which the Cost Function, (5), is minimum. This value of θ is taken as the predictive parameters, as shown in Fig 3.

Fig. 4. Predictive Algorithm obtained from the results of Linear Regression

The value of θ calculated above is used to make a Predictive algorithm that calculates the height and location of the obstacle based on the received power profile, as shown in Fig. 4.

Algorithm 1: Gradient Descent

Result: Predictive Parameters : θ
initialization θ = 0 ;
repeat until convergence {

$$\theta_i = \theta_i - \alpha \frac{\partial}{\partial \theta_i} J(\theta_0, \theta_1, ..., \theta_n) \quad \} \qquad (6)$$

III. RESULTS AND DISCUSSION

In this section, we present the simulation results for the proposed predictive VLC system with obstacles. The test set is used to calculate the accuracy of θ generated final value using gradient descent by using it to predict the height and location of the obstacle from the resultant RPP and comparing them to the actual values. The accuracy of location and height are calculated using (7) and (8), respectively, where the predicted values are calculated as $(\theta \times X_{test})$ and the actual values are Y_{test} and n is the number of data points in the test set. The accuracy values obtained in each given scenario are listed in Table 2, and the equation of accuracy is discussed below:

$$\text{Location Accuracy} = \frac{\sum_{i=1}^{n} \sqrt{(\hat{x} - x)^2 + (\hat{y} - y)^2}}{n} \qquad (7)$$

TABLE II
ACCURACY MATRIX

Obstacle	Setup A (One LED)		Setup B (Four LED)	
	Location accuracy (cm)	Height accuracy (cm)	Location accuracy (cm)	Height accuracy (cm)
Infinitely Thin Object	24.0120	16.5471 (99.9054%)	67.1274	14.7338 (99.9159%)
Object with finite Radius	3.5713	14.5927 (99.9135%)	5.4277	12.1816 (99.9293%)

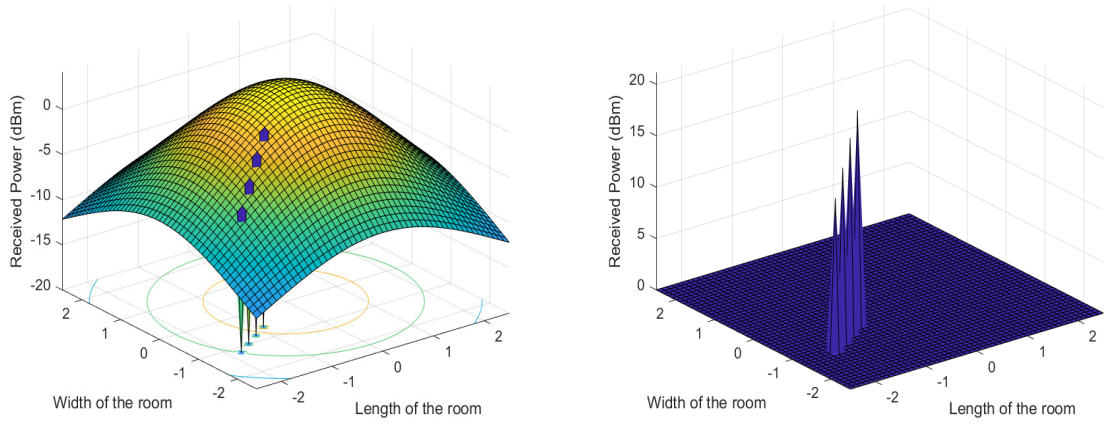

(a) Received Power Profile

(b) Difference b/w RPP with and without obstacle

Fig. 5. Infinitely thin obstacle is at (-0.9,-0.6) with height = 1.7 m (roughly 5'6") for single LED setup

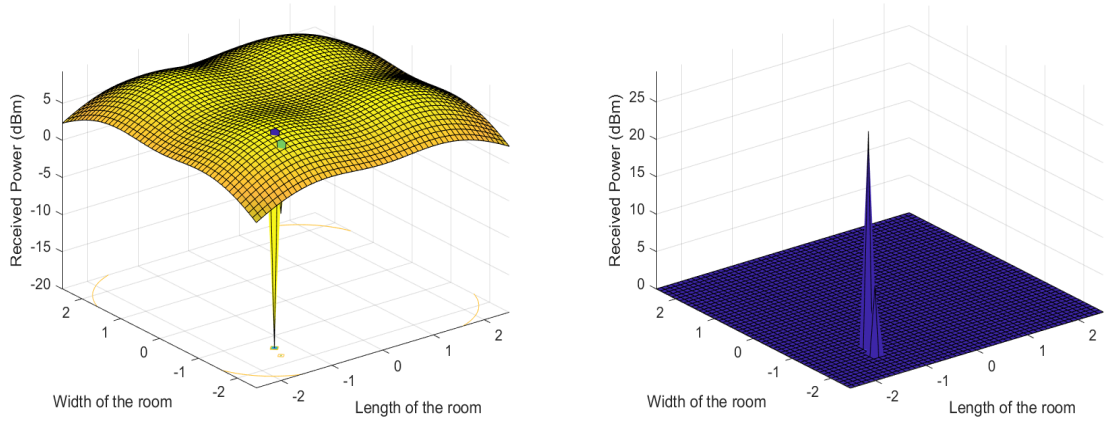

(a) Received Power Profile

(b) Difference b/w RPP with and without obstacle

Fig. 6. Infinitely thin obstacle is at (-1.3,-1.4) with height = 1.7 m (roughly 5'6") for four LED setup

$$\text{Height Accuracy} = \frac{\sum_{i=1}^{n} |\hat{h} - h|}{n} \tag{8}$$

$$\text{Accuracy}(\%) = \frac{\sum_{i=1}^{n} \frac{|\hat{h}-h|}{h}}{n} \tag{9}$$

where $\hat{x}$ and $\hat{y}$ are the predicted location of actual location x and y. Similarly, $\hat{h}$ is the predicted height of actual height h, and n is the total number of iteration.

A. Received Power Profile with infinitely thin object

The received power profile for an infinitely thin obstacle kept in a setup with a single LED and four LEDs can be observed in Figs 5 and 6, respectively.

The predicted value for location depends mainly on the nearest cartesian point, which is affected due to the presence of the obstacle. In the case of an infinitely thin obstacle, only the co-linear points with the obstacle and the LED are affected. Hence the nearest affected point may be quite far, which is the reason the accuracy of location is very low. The accuracy for height is also marginally lower for an infinitely thin obstacle because all the points that lie in the shadow of the obstacle are not affected. Hence, the full length of the shadow is not recorded.

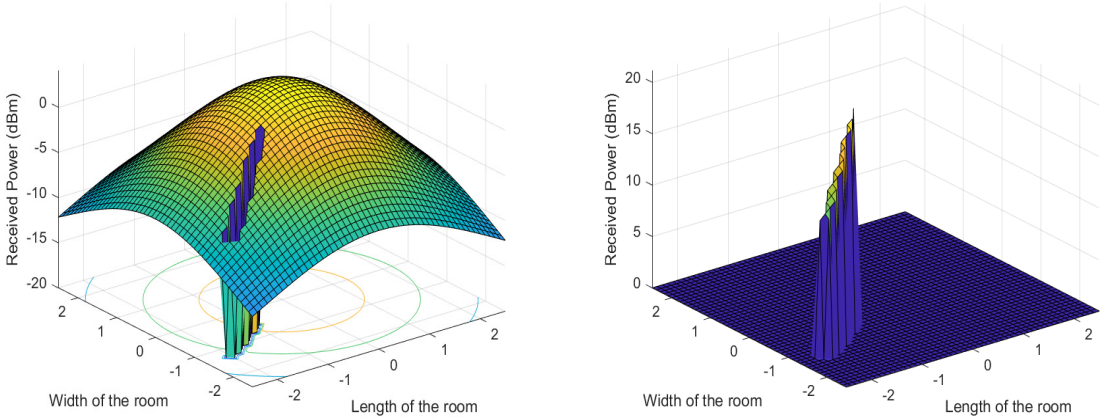

(a) Received Power Profile

(b) Difference b/w RPP with and without obstacle

Fig. 7. Obstacle having finite width(=0.05m) is at (-0.9,-0.6) with height = 1.7 m (roughly 5'6") for single LED setup

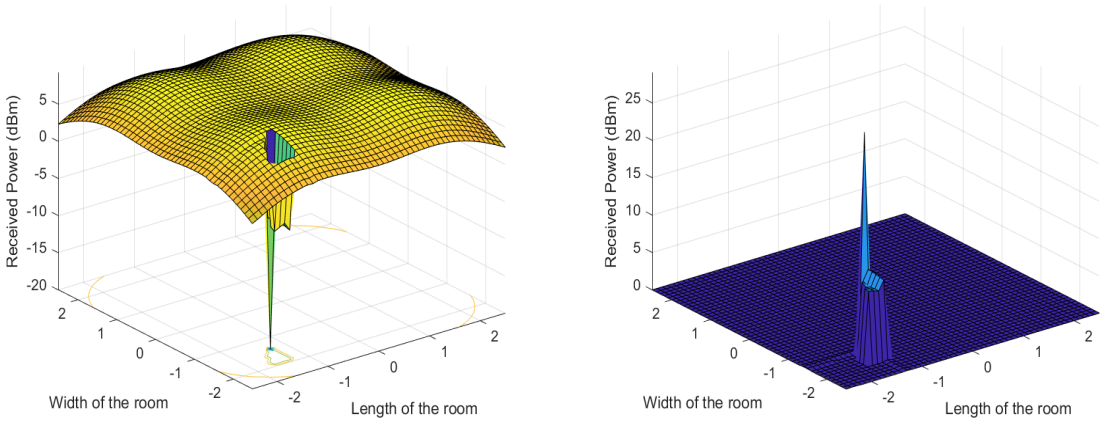

(a) Received Power Profile

(b) Difference b/w RPP with and without obstacle

Fig. 8. Obstacle having finite width(=0.05m) is at (-1.3,-1.4) with height = 1.7 m (roughly 5'6") for four LED setup

B. Received Power Profile with an object of finite radius

The received power profile for an obstacle with a radius of 0.05m kept in a setup with a single LED and with four LEDs can be seen in Figs 7 and 8, respectively.

From Table II, we can see that the accuracy of location increases in the case of an object having a finite radius (=0.05m). This is because the object now casts a definite shadow, and all the cartesian points lying in the shadow of the obstacle are affected in its presence. Similarly, the accuracy of height also increases as now the full length of the shadow is recorded.

The accuracy for location is lower in the case of a four LED setup because there is a different nearest affected point corresponding to each LED, which results in lower accuracy. On the other hand, the accuracy of height is greater for 4 LEDs because, in the case of a single LED, the shadow of an obstacle placed at the room's fringes goes beyond the room's boundary, and the full length cannot be measured. Whereas in the case of 4 LEDs, 4 different shadows are formed, and there is a higher correlation between the measured shadow and the actual shadow.

IV. CONCLUSION

This paper presented a predictive system for estimating the height and location of an obstacle. This is realized by an RSS based method using modulated LEDs. The system is simulated using an infinitely thin blockage and then with a blockage having a constant finite radius (= 0.05m). Based on the results of the simulation, a predictive algorithm is built using multivariate linear regression. The accuracy of the predictive algorithm developed is reasonably high as it predicts the location of the obstacle within 5 cm and the height within 15 cm.

REFERENCES

[1] M. E. Rida, F. Liu, Y. Jadi, A. A. A. Algawhari, and A. Askourih, "Indoor location position based on bluetooth signal strength," in *2015 2nd International Conference on Information Science and Control Engineering*. IEEE, 2015, pp. 769–773.

[2] C. Yang and H.-R. Shao, "WiFi-based indoor positioning," *IEEE Communications Magazine*, vol. 53, no. 3, pp. 150–157, 2015.

[3] X.-Y. Lin, T.-W. Ho, C.-C. Fang, Z.-S. Yen, B.-J. Yang, and F. Lai, "A mobile indoor positioning system based on ibeacon technology," in *2015 37th Annual International Conference of the IEEE Engineering in Medicine and Biology Society (EMBC)*. IEEE, 2015, pp. 4970–4973.

[4] R. Harle, "A survey of indoor inertial positioning systems for pedestrians," *IEEE Communications Surveys & Tutorials*, vol. 15, no. 3, pp. 1281–1293, 2013.

[5] C.-H. Huang, L.-H. Lee, C. C. Ho, L.-L. Wu, and Z.-H. Lai, "Real-time RFID indoor positioning system based on kalman-filter drift removal and heron-bilateration location estimation," *IEEE Transactions on Instrumentation and Measurement*, vol. 64, no. 3, pp. 728–739, 2014.

[6] N. U. Hassan, A. Naeem, M. A. Pasha, T. Jadoon, and C. Yuen, "Indoor positioning using visible LED lights: A survey," *ACM Computing Surveys (CSUR)*, vol. 48, no. 2, pp. 1–32, 2015.

[7] A. M. Vegni and M. Biagi, "An indoor localization algorithm in a small-cell LED-based lighting system," in *2012 International Conference on Indoor Positioning and Indoor Navigation (IPIN)*. IEEE, 2012, pp. 1–7.

[8] P. Prasithsangaree, P. Krishnamurthy, and P. Chrysanthis, "On indoor position location with wireless lans," in *The 13th IEEE international symposium on personal, indoor and mobile radio communications*, vol. 2. IEEE, 2002, pp. 720–724.

[9] M. Yoshino, S. Haruyama, and M. Nakagawa, "High-accuracy positioning system using visible LED lights and image sensor," in *2008 IEEE Radio and Wireless Symposium*. IEEE, 2008, pp. 439–442.

[10] X. Zhang, J. Duan, Y. Fu, and A. Shi, "Theoretical accuracy analysis of indoor visible light communication positioning system based on received signal strength indicator," *Journal of Lightwave Technology*, vol. 32, no. 21, pp. 3578–3584, 2014.

[11] Z. Vatansever and M. Brandt-Pearce, "Visible light positioning with diffusing lamps using an extended kalman filter," in *2017 IEEE Wireless Communications and Networking Conference (WCNC)*. IEEE, 2017, pp. 1–6.

[12] Y. Gu, A. Lo, and I. Niemegeers, "A survey of indoor positioning systems for wireless personal networks," *IEEE Communications surveys & tutorials*, vol. 11, no. 1, pp. 13–32, 2009.

[13] S. Shawky, M. A. El-Shimy, Z. A. El-Sahn, M. R. M. Rizk, and M. H. Aly, "Improved vlc-based indoor positioning system using a regression approach with conventional rss techniques," in *2017 13th International Wireless Communications and Mobile Computing Conference (IWCMC)*, 2017, pp. 904–909.

[14] F. R. Gfeller and U. Bapst, "Wireless in-house data communication via diffuse infrared radiation," *Proceedings of the IEEE*, vol. 67, no. 11, pp. 1474–1486, 1979.

[15] M. Jacob, S. Priebe, T. Kürner, M. Peter, M. Wisotzki, R. Felbecker, and W. Keusgen, "Fundamental analyses of 60 ghz human blockage," in *2013 7th European Conference on Antennas and Propagation (EuCAP)*. IEEE, 2013, pp. 117–121.